Mechanical Systems and Signal Processing ▮ (▮▮▮▮) ▮▮▮–▮▮▮

Contents lists available at SciVerse ScienceDirect

Mechanical Systems and Signal Processing

journal homepage: www.elsevier.com/locate/ymssp

Autoregressive statistical pattern recognition algorithms for damage detection in civil structures

Ruigen Yao*, Shamim N. Pakzad

Department of Civil and Environmental Engineering, Lehigh University, Bethlehem, PA 18015, USA

ARTICLE INFO

Article history:
Received 15 January 2011
Received in revised form
16 February 2012
Accepted 21 February 2012

Keywords:
Structural health monitoring
Damage detection
Statistical pattern recognition
Time series analysis
Autoregressive modeling
Monte Carlo method

ABSTRACT

Statistical pattern recognition has recently emerged as a promising set of complementary methods to system identification for automatic structural damage assessment. Its essence is to use well-known concepts in statistics for boundary definition of different pattern classes, such as those for damaged and undamaged structures. In this paper, several statistical pattern recognition algorithms using autoregressive models, including statistical control charts and hypothesis testing, are reviewed as potentially competitive damage detection techniques. To enhance the performance of statistical methods, new feature extraction techniques using model spectra and residual autocorrelation, together with resampling-based threshold construction methods, are proposed. Subsequently, simulated acceleration data from a multi degree-of-freedom system is generated to test and compare the efficiency of the existing and proposed algorithms. Data from laboratory experiments conducted on a truss and a large-scale bridge slab model are then used to further validate the damage detection methods and demonstrate the superior performance of proposed algorithms.

1. Introduction

Structural health monitoring (SHM) [1] has been proposed by the civil engineering research community as an economical and possibly more reliable solution to infrastructure condition assessment. SHM can be realized by collecting data from a sensor network installed on the monitored structure and then processing the measurements for structural condition evaluation. A number of algorithms have been developed by different research groups to extract critical structural information from the measured data. Conventional methods focus on direct estimation of structure's physical parameters such as modal properties, which often require a numerical model of the structure [2–5]. While these physical properties are easy concepts for interpretation, most of them are computationally intensive to estimate, and in a lot of cases fail to identify significant local damage even with a dense sensor network. Recently, statistical pattern recognition techniques (SPR) [6] are being investigated in hope of finding a more efficient algorithm for distributed damage detection.

Statistical pattern recognition techniques (Fig. 1) have long been applied to speech recognition [7], identifying logical information from image documents [8,9], reading DNA sequences in bioinformatics [10] and problems in many other domains that require artificial cognitive assistance. Their ability to process large volumes of information produced via continuous and/or multichannel sensing is very beneficial, and in addition, these techniques are adaptable to most fields of

* Corresponding author.
E-mail addresses: ruy209@Lehigh.edu (R. Yao), pakzad@Lehigh.edu (S.N. Pakzad).

0888-3270/$ - see front matter © 2012 Elsevier Ltd. All rights reserved.
doi:10.1016/j.ymssp.2012.02.014

Please cite this article as: R. Yao, S.N. Pakzad, Autoregressive statistical pattern recognition algorithms for damage detection in civil structures, Mech. Syst. Signal Process. (2012), doi:10.1016/j.ymssp.2012.02.014

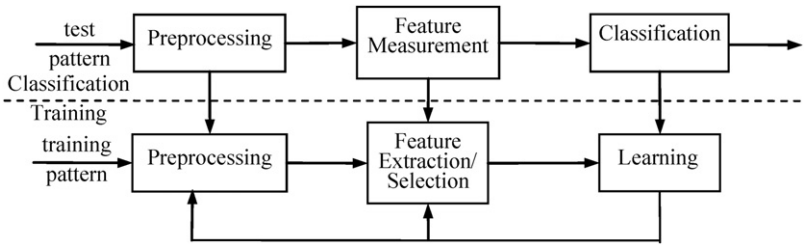

Fig. 1. The general procedure of statistical process control [6].

applied science as they are basically mathematical tools. The range of application of these techniques continues to expand to many new areas of natural and social sciences and engineering.

The SPR paradigm for vibration-based SHM, proposed in [11], consists of four tasks: (1) operational evaluation; (2) data acquisition; (3) feature selection and data compression; and (4) statistical model development. This paradigm essentially focuses on the interdependence between structural data collection details and statistical data analysis procedures and their application.

The four components of this paradigm have all been studied in the past, and amongst them the task of statistical decision making has recently received increasing attention. References [12–17] presented the application of hypothesis testing and clustering techniques to damage classification and reported satisfactory results. The feature extraction methods adopted in these papers are based on AR/ARX/ARMA (Autoregressive/Autoregressive with exogenous input/Autoregressive with moving average [18,19]) modeling. Several other studies further explored the effectiveness of autoregressive damage indicators [20–29] by making changes to data cleansing techniques, using different classification algorithms, and trying the statistical method on different types of simulated and real structures.

Feature extraction and statistical boundary construction are two crucial factors concerning the effectiveness of a SPR algorithm. Ever since the concept of SPR was introduced in the structural damage detection field, research has been focused on how to obtain a sensitive feature and a reliable damage threshold. In the context of statistical pattern recognition, each pattern is represented by a feature vector. Familiar concepts from statistics are then utilized to construct boundaries between different classes based on analyzing a group of patterns whose class properties are known beforehand. This process is generally known as training of the classification machine or threshold construction. Unidentified patterns can then be classified by the established statistical machine.

Even though the implementation of SPR does not require the adopted features to have an explicit physical meaning, the features that represent the underlying structural physics are preferred for structural monitoring if their performance is adequate, from the point of view that they can provide more effective insight into the condition of the structure. As an example of such features, the parameters of an input–output based ARX model for the LTI (linear time-invariant) systems represent the structural response under white Gaussian excitation at an arbitrary location. AR/ARX/ARMA based damage indicators are thus preferable features compared with those purely statistical indices of structural vibration responses such as kurtosis (a statistics measuring the sharpness of sample distribution) and principal components (a linear combination of observations from multiple channels such that the results possess maximum variance, therefore conveying the most information). The existing AR/ARX/ARMA methods for damage detection are based on monitoring of model residual variances and model parameter vectors. Though theoretically justified, they only reflect possible changes in certain aspects of the model, and may not be the most effective ways to apply AR/ARX/ARMA based damage detection. In addition, their robustness to noise has been largely left unexamined. In this paper two algorithms using different features and statistical decision strategies will be proposed along with a brief investigation into the damage sensitivity of AR model coefficients and residuals. The performance of new algorithms will be compared to that of the existing methods through numerical and laboratory experiments. Also, a modification to the data-driven scheme for damage threshold construction using Mahalanobis distance features is introduced to improve the performance of the algorithm.

The organization of this paper is in Sections 6. In Section 2, a brief summary of current SPR algorithms using AR/ARX models is presented. An analysis on how the structural change and measurement noise can affect the performance of autoregressive-based damage features is introduced in Section 3. The limitations of available methods are highlighted and new algorithms based on Ljung-Box statistic and AR spectra are proposed. To compare the performances of existing versus the proposed algorithms, both methods are applied to a numerical example in Section 4 and to the data collected from laboratory experiments in Section 5 for further evaluation.

2. SPR algorithms using AR/ARX based features

Many SPR algorithms only look at a certain aspect of AR/ARX models for input features. Two most commonly adopted features are model residuals and model coefficients.

Please cite this article as: R. Yao, S.N. Pakzad, Autoregressive statistical pattern recognition algorithms for damage detection in civil structures, Mech. Syst. Signal Process. (2012), doi:10.1016/j.ymssp.2012.02.014

2.1. Model residuals as damage indicator

An AR(p) model can be written as:

$$x(t) = \sum_{j=1}^{p} \phi_{xj} x(t-j) + \epsilon_x(t). \tag{1}$$

In this equation $x(t)$ is the discrete-time autoregressive signal, $\epsilon_x(t)$ is the random error, ϕ_{xj} denotes the AR coefficients, and p is the order of the model.

An ARX model is similar to an AR model in structure, only there is an additional regression term on the right side of the equation for an external input $e(t)$:

$$x(t) = \sum_{i=1}^{a} \alpha_i x(t-i) + \sum_{j=0}^{b} \beta_j e(t-j) + \epsilon_x(t). \tag{2}$$

The one-step prediction error of an AR/ARX model over a dataset is generally referred to as model residuals. In application, damage indicators can be certain characteristics of the residuals obtained by fitting a model from baseline $x(t)$ to a dataset $y(t)$ collected from an unknown state.

$$\begin{aligned} &\text{AR analysis}: \ \epsilon_y(t) = y(t) - \sum_{j=1}^{p} \phi_{xj} y(t-j), \\ &\text{ARX analysis}: \ \epsilon_y(t) = y(t) - \sum_{i=1}^{a} \alpha_i y(t-i) - \sum_{j=1}^{b} \beta_j e_y(t-j). \end{aligned} \tag{3}$$

In [13], the ARX model residuals from strain gage data from a patrol boat are used to report damage. Note that since the input information is not available in this case, a two-stage analysis is adopted. First an AR(p) model is fitted to all signal segments to obtain the residuals and AR coefficients. Then the baseline data segment $x(t)$ whose AR coefficients are closest to that of the unidentified data $y(t)$ is selected, and an ARX (a,b) model is constructed from $x(t)$ using its AR residuals as exogenous input. Hence, ARX residual sequences ϵ_x and ϵ_y can be obtained, respectively from $x(t)$ and $y(t)$ using the baseline model. The ratio $\sigma(\epsilon_y)/\sigma(\epsilon_x)$ is defined as the damage-sensitive feature in this case. Here $\sigma(\cdot)$ denotes the standard deviation of a sequence. An increase in the values of damage indicator is observed as the system became damaged.

In another study [14] on damage identification in a mass-spring-damper system using acceleration response, similar methodology is used for feature extraction but a more statistically rigorous approach is employed for damage threshold construction. The selected damage index is $\sigma^2(\epsilon_y)/\sigma^2(\epsilon_x)$, which should follow an F-distribution under the Gaussian assumption of residuals. A modified hypothesis test is used to set the damage threshold.

A successful application of AR residuals in detecting structural change in a progressively damaged concrete bridge column is reported in [12]. Acceleration measurements are collected from a single sensor mounted on the model. A healthy-state dataset is used to train a baseline AR model, which is fitted to both training and unknown state data to produce AR residual sequences. These sequences are divided into subgroups of size 4, and within-subgroup mean ($\bar{x}$) and standard deviation (S) are monitored using statistical process control chart. The upper/lower control limits of the charts are determined from baseline data residuals (Table 1); when the system is damaged, it is expected that a large portion of charted values will go beyond the limits.

2.2. AR coefficients as damage indicators

In the same paper [13] where AR-ARX residuals are used to capture damage, an outlier analysis is performed for the AR coefficients. The distance measure adopted for novelty evaluation is Mahalalobis distance [30]:

$$D_\xi = (x_\xi - \bar{x})\Sigma^{-1}(x_\xi - \bar{x}), \tag{4}$$

where x_ξ is the potential outlier vector, $\bar{x}$ is the mean vector of the baseline sample features, and Σ is the sample covariance matrix.

Table 1
Formulas for upper/lower bound calculation of the two control charts [12].

	Upper bound	Lower bound	Center line
$\bar{x}$ chart	$z_{\alpha/2} s_p/\sqrt{n}$	$-z_{\alpha/2} s_p/\sqrt{n}$	0
S chart	$\bar{S}\sqrt{\chi^2_{1-\alpha/2,n-1}/(n-1)}$	$\bar{S}\sqrt{\chi^2_{\alpha/2,n-1}/(n-1)}$	s_p

$^{**}\boldsymbol{s_p}$ is the square root of pooled variance of subgroups in the baseline residual set, and $\boldsymbol{z_\alpha}$ represents the α quantile of the standard normal distribution. $^{**}\boldsymbol{\chi^2_{p,n}}$ denotes the pth quantile of a Chi-square random variable with n degrees-of-freedom.

Please cite this article as: R. Yao, S.N. Pakzad, Autoregressive statistical pattern recognition algorithms for damage detection in civil structures, Mech. Syst. Signal Process. (2012), doi:10.1016/j.ymssp.2012.02.014

Mahalanobis distance is defined from the deviation statistics; a normal Gaussian statistical population in p-variants is usually described by a p- dimensional frequency distribution:

$$f(x,\mu,\Sigma)=\frac{1}{(2\pi)^{p/2}|\Sigma|^{1/2}}\exp\left(\frac{1}{2}(x-\mu)^T\Sigma^{-1}(x-\mu)\right). \tag{5}$$

where x is the p-dimensional Gaussian Random Vector, μ is its expectation, and Σ is its covariance matrix. When data from a structural state that differs from the baseline is tested, Mahalanobis distance value for AR coefficients is expected to increase substantially. Monte Carlo Simulation was employed for damage threshold construction: feature vectors with components drawn independently from a standard normal distribution are generated, and then their Mahalanobis distance values are computed and arranged in descending order. The threshold is set at the point beyond which 1% or 5% values occur.

Mahalanobis distance is also adopted for damage detection in an experimental research described in [25], where AR modeling is applied to the free decay response produced via random decrement technique, instead of the raw ambient response.

3. Proposed damage detection algorithms based on time series analysis

Though in several studies, AR models have been employed for feature extraction to detect structural damage, they mainly emphasized on development and validation of the SPR method and did not focus on examining their effectiveness for structural monitoring by sensitivity analysis. In this section the sensitivity of AR model properties as damage indicators will be inspected, and from the analysis result new autoregressive features based on model residuals and parameters are proposed.

Damage detection is essentially an inverse problem that attempts to diagnose the system using the input (excitation) and output (structural response) records. Since in most practical situations input information is difficult to obtain, a convenient, yet in most cases justifiable assumption is made that the excitation is white noise. Theoretically, the structural vibration response under such loading can be treated as an ARMA(p,q) process, with a corresponding z-transfer function [31] as shown in Eq. (6):

$$X(z)=\frac{1-\theta_1 z^{-1}-\theta_2 z^{-2}-\cdots-\theta_p z^{-q}}{1-\phi_1 z^{-1}-\phi_2 z^{-2}\cdots-\phi_p z^{-p}}. \tag{6}$$

In this equation, the auto regressive (AR) coefficients, $\{\phi_i\}$, are determined by structural properties, and the moving average (MA) coefficients, $\{\theta_i\}$ are affected by both the structural condition and excitation. The location of the zeros of the process, determined by the MA coefficients, can be easily affected by even a slight measurement noise content that introduces a rippled noise floor to the signal spectrum. In Fig. 2, the two ARMA models have the same AR coefficients but different MA coefficients. The blue and red lines are the Welch's periodogram plots from data generated from the two models. The results are presented as an empirical proof that the zero positions (which is related to the MA coefficients) of a system cannot be reliably inferred from noise contaminated signals. As such, the ARMA models, despite their higher computational cost, do not yield a performance superior to AR models in many applications. Therefore, using AR models is a preferable choice for constructing an efficient and effective damage detection algorithm that will work for online or distributed structural monitoring. In the remainder of this paper, the discussion will be limited to AR models.

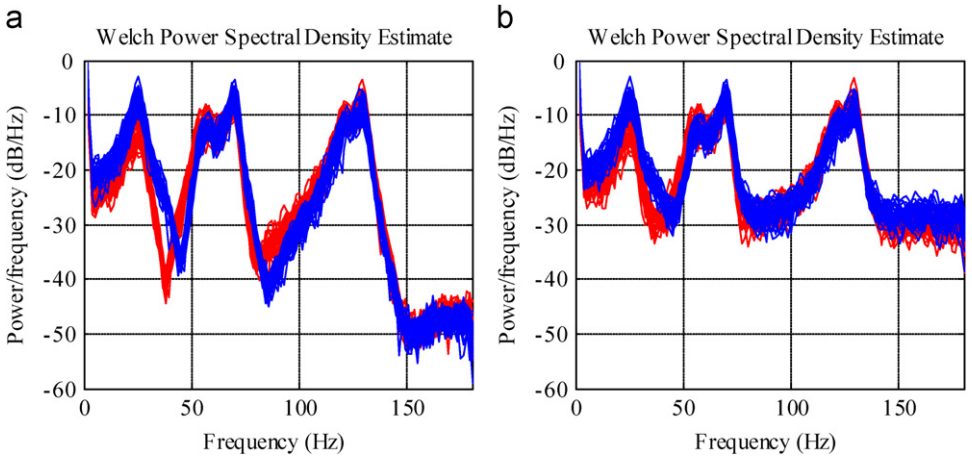

Fig. 2. Sample spectrum pots from 50 simulations of two ARMA processes: (a) constructed from noise-free sample; (b) constructed from samples with 6.5% noise added. (For interpretation of the references to color in this figure legend, the reader is referred to the web version of this article.)

Please cite this article as: R. Yao, S.N. Pakzad, Autoregressive statistical pattern recognition algorithms for damage detection in civil structures, Mech. Syst. Signal Process. (2012), doi:10.1016/j.ymssp.2012.02.014

3.1. Damage detection using autocorrelation function (ACF) of the residuals

From the definition of the AR model it is clear that if the autoregressive model used to filter an AR process is exactly the same as its underlying structure, then the produced model residuals should be the same as $\epsilon_x(t)$ in Eq. (1). Otherwise, the residual sequence will resemble an ARMA process instead of being a white noise.

Reference [32] proposed a statistic to measure the difference between residual series and identically and independently distributed (i.i.d.) noise:

$$Q = n(n+2)\sum_{j=1}^{h}\frac{\rho_j^2}{n-j}, \tag{7}$$

where n is the sample size, h is the number of lags, and ρ_j is the autocorrelation at the jth lag. Since this Q–statistic follows a χ^2 distribution under the normality assumption of the input, a statistical test can be devised at significance levelα, by setting the rejection threshold at $\chi^2_{1-\alpha,h}$, which is the α– quantile of the χ^2 distribution with h degrees-of-freedom.

This so-called Ljung-Box test is yet a novel statistical approach in the civil engineering domain. Nonetheless, it seems an attractive alternative for damage detection to residual-variance based methods, and will be applied in conjunction with AR modeling in Sections 4 and 5. In the rest of this subsection, an analytical result will be provided on the sensitivity of residual ACF to structural damage. Here, structural damage is represented as a change in AR coefficients (indirect structural parameters), rather than parameters with a clear physical meaning (mass, stiffness, etc.).

Assume that the structural vibration response at a certain location can be described by a univariate AR(p) model:

$$x(t)-\phi_1 x(t-1)-\phi_2 x(t-2)-\cdots-\phi_p x(t-p)=e(t). \tag{8}$$

The corresponding z-transfer function is (p is always an even number, as the structural poles always appear in pairs as conjugates):

$$\Phi(z)=\frac{E(z)}{X(z)}=\frac{1}{1-\phi_1 z^{-1}-\phi_2 z^{-2}\cdots-\phi_p z^{-p}}=\frac{1}{(1-a_1 z^{-1})(1-a_1^* z^{-1})(1-a_2 z^{-1})(1-a_2^* z^{-1})\cdots(1-a_{p/2} z^{-1})(1-a_{p/2}^* z^{-1})}, \tag{9}$$

which is an all-pole expression. It can be shown that the poles of a discretized MDOF structure are related to its eigenfrequencies (ω_i) and damping ratios (ζ_i) through the following expression [31]:

$$a_i,\ a_i^* = e^{-\zeta_i\omega_i T_s \pm \omega_i\sqrt{1-\zeta_i^2}T_s},\quad i:\ \text{the mode order} \tag{10}$$

In Eq. (10), T_s is the data sampling frequency. Hence in the subsequent derivations, damage will be represented by a shift in the position of system poles. To simplify the discussion, suppose the model only differs from the data structure in the first pair of conjugate poles, a_1 and a_1^*, by a value of Δa_1 and Δa_1^*, where $(\Delta a_1)^* = \Delta a_1^*$. The z-transfer function of the residual sequence from the new structural state can be expressed as:

$$E'(z)=\frac{[1-(a_1+\Delta a_1)z^{-1}][1-(a_1^*+\Delta a_1^*)z^{-1}]}{(1-a_1 z^{-1})(1-a_1^* z^{-1})}E(z). \tag{11}$$

Eq. (11) can be written in the time domain as

$$(1-a_1B)(1-a_1^*B)e'(t)=[1-(a_1+\Delta a_1)B][1-(a_1^*+\Delta a_1^*)B]e(t),$$

$$e'(t)=\sum_{n=0}^{\infty}(a_1B)^n\sum_{m=0}^{\infty}(a_1^*B)^m[1-(a_1+\Delta a_1)B][1-(a_1^*+\Delta a_1^*)B]e(t)=e(t)+\left[\sum_{n=0}^{\infty}(a_1B)^n(-\Delta a_1^*B)+\sum_{m=0}^{\infty}(a_1^*B)^m(-\Delta a_1B)\right]e(t)$$

Here B stands for the backshift operator, i.e., $Bp[n]=p[n-1]$. Considering changes in all pole pairs,

$$e'(t)=e(t)+\sum_{k=1}^{p}\left[\sum_{n=0}^{\infty}(a_1B)^n(-\Delta a_1^*B)+\sum_{m=0}^{\infty}(a_1^*B)^m(-\Delta a_1B)\right]e(t). \tag{12}$$

This result is obtained under the assumption that the deviation of the model from its original state is very small.

From Eq. (12) it is clear that as the model deviates from the baseline, the residuals will be the sum of a white noise sequence and a number of attenuated auto-regressive terms. As a result, an increase will be observed in its standard deviation, and its autocorrelation function will start showing non-zero values at different time lags. A simple derivation leads to an expression for the ACF of $e'(t)$:

$$R_{e'}(t)=\sigma_e^2\left\{\delta(t)+\sum_{k=1}^{p}(-\Delta a_1^*-\Delta a_1)\delta(t-1)+\sum_{k=1}^{p}\sum_{l=0}^{p}\left[\frac{(\Delta a_k\Delta a_l)^* a_l^t}{1-(a_k a_l)^2}+\frac{\Delta a_k\Delta a_l a_l^{*t}}{1-(a_k^* a_l^*)^2}+\frac{\Delta a_k^*\Delta a_l a_l^{*t}}{1-(a_k a_l^*)^2}+\frac{\Delta a_k\Delta a_l^* a_l^t}{1-(a_k^* a_l)^2}\right]\right\}, \tag{13}$$

where σ_e^2 is the noise variance. In Eq. (13) high order terms are not omitted because the poles of a physical structure are generally close to the unit circle, thus making the value of the denominators small. The damage detection methods that were examined in Section 2 are based on mean and standard deviation control charts on grouped residuals and F-test on residual variance. Eq. (13) suggests that more sensitive statistical features can be found by taking into consideration the change of the entire ACF, instead of focusing only on the change in residual standard deviation.

Please cite this article as: R. Yao, S.N. Pakzad, Autoregressive statistical pattern recognition algorithms for damage detection in civil structures, Mech. Syst. Signal Process. (2012), doi:10.1016/j.ymssp.2012.02.014

3.2. Damage detection using AR model spectrum

Corresponding spectrum plot can be constructed given an AR model:

$$S_{\mathrm{AR}}^{(p)}(\omega)=\frac{\sigma_e^2}{|\phi(e^{j\omega})|^2}=\frac{\sigma_e^2}{|\sum_{k=0}^{p}\phi_k e^{-j\omega k}|^2} \tag{13}$$

In this paper σ_e^2 is not calculated and set to 1, since its value can be determined by excitation level.

It is proposed here that Cosh spectral distance [4,33] based on AR spectrum estimates be used as a more stable damage index than Mahalanobis distance of AR coefficients:

$$C(S,\bar{S})=\frac{1}{2N}\sum_{j=1}^{N}\left[\frac{S(\omega_j)}{\bar{S}(\omega_j)}-\log\frac{S(\omega_j)}{\bar{S}(\omega_j)}+\frac{\bar{S}(\omega_j)}{S(\omega_j)}-\log\frac{\bar{S}(\omega_j)}{S(\omega_j)}-2\right]. \tag{14}$$

In Eq. (14), $S(\omega_j)$ is the Power Spectral Density to be examined, and $\bar{S}(\omega_j)$ is the average of the spectra estimates from baseline samples. When the system is damaged, the Cosh distance value should increase. Since no theoretical probability distribution is available for this statistic, damage threshold will be determined numerically from the baseline. Specifics on threshold construction will be introduced in the next section.

Structural damage will influence the values of the AR coefficients obtained from autoregressive modeling on the vibration responses. A desirable feature is one that is sensitive to the damage, but not very sensitive to other non-relevant factors. A theoretical solution on the feature sensitivity would require not only a thorough inspection of the numerical estimation algorithm used, but also evaluation of finite sample number effect and complicated statistical distributions. Therefore, numerical simulations are adopted to investigate this subject. Each simulation consists of 50 runs, in which sample data are generated from an ARMA (10, 6) process with white noise added. In Fig. 3, the first row shows how the coefficient and spectrum estimates respond to the change in signal noise level, the second row shows how these estimates are affected by a slight variation in the positions of two zeros of the ARMA process (as reflected in the difference between the two thin blue lines), and the third row shows their responses to change in the values of two poles of the ARMA process. In all estimations the AR order is set at 16.

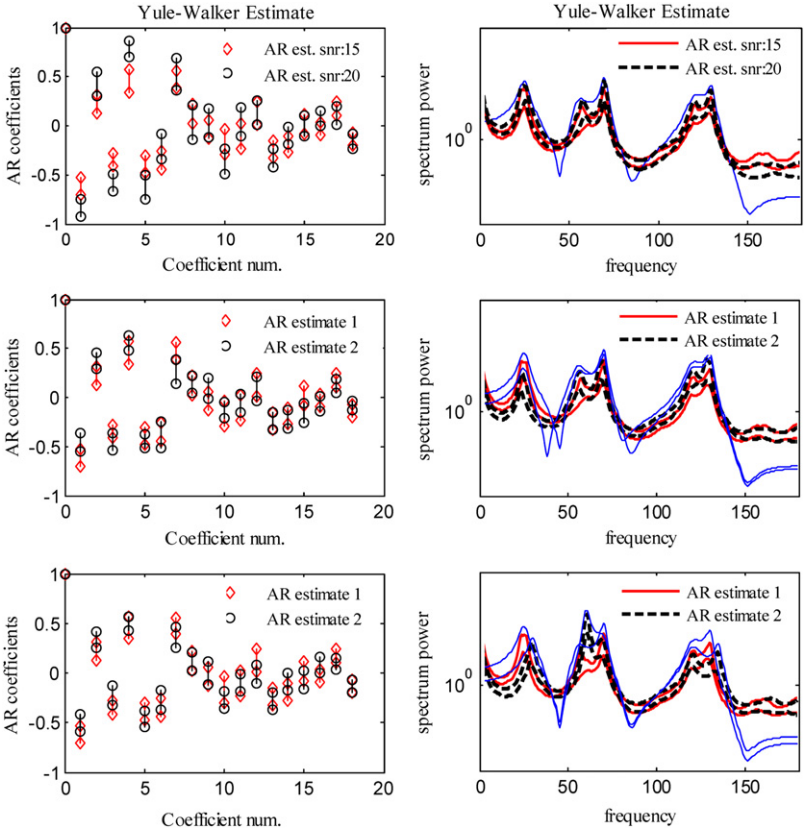

Fig. 3. The estimation interval of AR coefficient and envelope of spectrum estimates over 50 simulations. 'snr' is the abbreviation for signal-to-noise ratio. In all the spectrum plots, the thin blue lines(s) represents the spectrum of underlying model(s). (For interpretation of the references to colour in this figure legend, the reader is referred to the web version of this article.)

Please cite this article as: R. Yao, S.N. Pakzad, Autoregressive statistical pattern recognition algorithms for damage detection in civil structures, Mech. Syst. Signal Process. (2012), doi:10.1016/j.ymssp.2012.02.014

As can be seen in the second and third row of Fig. 3, the signs and values of AR coefficients are sensitive to the change in position of zeros and noise ratio, and especially to the latter; when the noise level is raised slightly, substantial variation happens in the value of first six AR coefficients. The Mahalanobis distance measure mentioned before is implicitly based on the assumption that the estimated coefficients are Gaussian random vectors, which is only true asymptotically when the underlying process is strictly AR(p); see [17] for details. When such variations are considered, the general 'shape' of the coefficient cluster may be easily affected and thus render this feature not robust with respect to variation due to environmental factors.

Judging from the plots, the AR spectrum estimate seems a more reliable feature compared to the coefficients. This feature is not greatly affected by noise level change, and has the desired feature of being more sensitive to shift in poles than zeros (considering the logarithmic plot scale that magnifies the difference between small values). No explicit reasoning is available now to account for this phenomenon, but the interaction between polynomial coefficients and roots is complicated when the polynomial order is high; sometimes a slight change in one corresponds to great variation in the other.

4. Numerical implementation of the statistical algorithms

To examine the effectiveness of both the old and new algorithms, a four degree-of-freedom mass-spring-damper system (Fig. 4), subjected to white noise excitation is simulated using MATLAB. Two sets of acceleration measurements are collected at all nodes from the healthy structure. Then damage is simulated by reducing the stiffness of the spring between nodes 3 and 4 by 20%, and two additional sets of acceleration measurements are obtained from the damaged structure. Figs. 5 and 6 display the results from different statistical algorithms. In all these statistical tests, one dataset (dataset 2) from the undamaged condition is used to establish the baseline, and the other (dataset 1) for false-positive testing. The other two sets from the damaged state are used to demonstrate each method's damage detection performance. Each dataset consists of 3000 points. The order of AR models is determined by using Akaike's Information Criterion (AIC) [19].

Damage is clearly indicated by both the $\bar{x}$ control chart and Q-statistic trace plot (Fig. 5). The AR model order used in control chart construction is 28, the subgroup size is 4. The maximum lag number for Q-statistic evaluation is 25. The significance level of the threshold is 5%. The classification result using S-control chart is not satisfactory, possibly due to the fact that the residuals are not completely uncorrelated. Q-statistic trace plots are the more sensitive features, where the values from the damaged state significantly increase as model order increases. Such large differences have compensated the imperfection of having the false positive trace lying above the threshold. Note that as the AR order increases, the model overfits dataset 2, thus making the difference in Q-statistic value obtained from dataset 1 and dataset 2 greater. Another interesting point observed is that as model order increases, the false positive trace becomes quite flat, while the two damaged state traces are fluctuating.

Fig. 4. The simulated 4 DOF mass-spring-damper system.

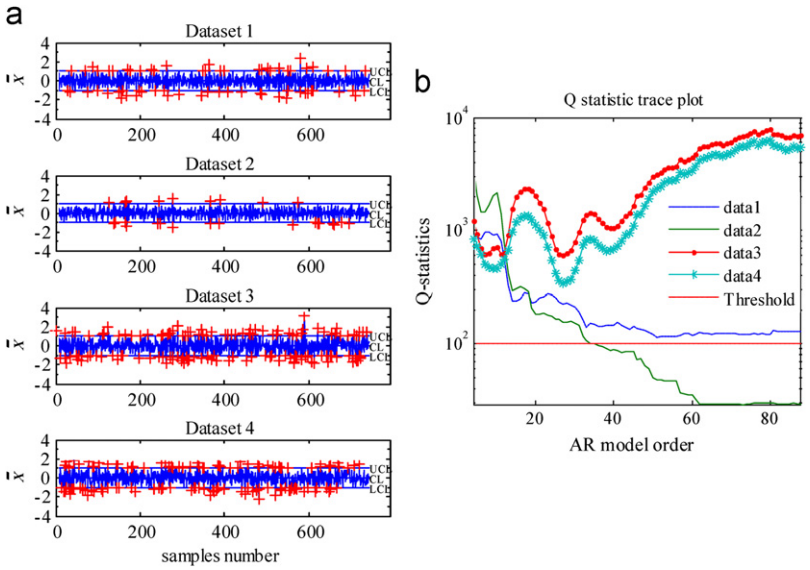

Fig. 5. Damage classification results in the numerical case, by (a) $\bar{x}$ control chart and (b) Ljung-Box test statistic; all data are acquired from node 3.

Please cite this article as: R. Yao, S.N. Pakzad, Autoregressive statistical pattern recognition algorithms for damage detection in civil structures, Mech. Syst. Signal Process. (2012), doi:10.1016/j.ymssp.2012.02.014

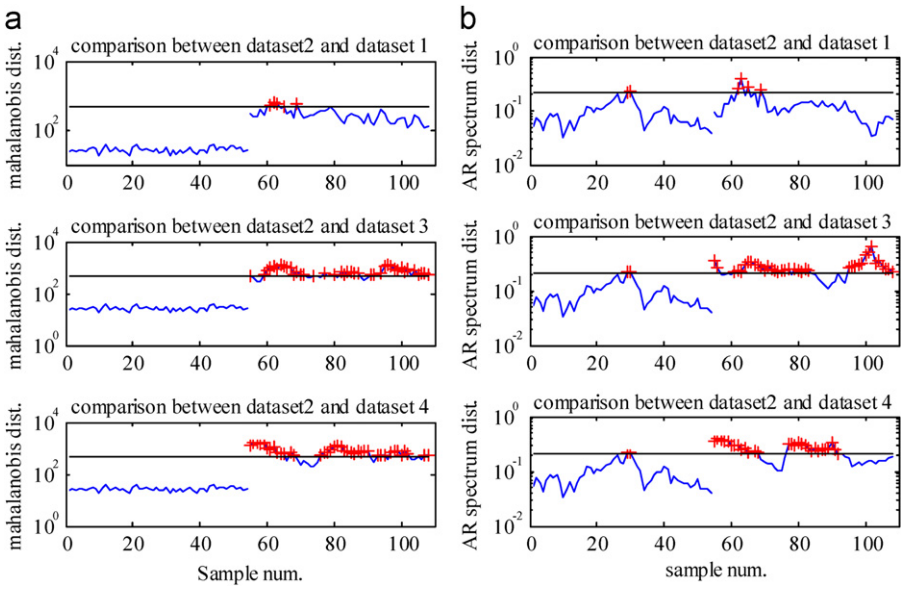

Fig. 6. Damage classification results in the numerical case, (a) Mahalanobis distance and (b) Cosh spectral distance measure.

In Fig. 6, The AR model order employed is 28, and each dataset is segmented into a group of 350-point long pieces with 300-point overlap between successive parts. The significance level of the threshold is 5%. The number of FFT (fast Fourier Transform) points is 256. It can be seen that the Mahalanobis distance feature is not robust with respect to variation due to environmental factors, and careful consideration is given to the corresponding damage threshold construction so that a balance can be reached between the amount of false alarms and missed damage cases. The Monte Carlo method described in the previous case yields poor results since it produces such a high threshold value that all features, whether from damaged or undamaged state, fall below the threshold. Also, this technique is not theoretically justified: It has been proved that if the signal is really an AR process, then any regular coefficients estimator $\{\phi_{xj}\}$ from the signal is asymptotically unbiased and normally distributed with covariance matrix $\sigma_e^2\Gamma_p^{-1}$, where $\Gamma_p=[\gamma(i-j)]_{i,j=1,\ldots,p}$ (γ is the signal autocorrelation function) [19]. Another intuitive method is to simulate random Gaussian vectors based on the covariance matrix estimated from baseline samples, but due to the feature robustness problem described before, the rate of false alarms tends to be high for this method.

Finally the method adopted is the data-driven cross-one-validation, a method that 'let the data speak for itself'. First a segment is cut at a random time point from the baseline sequence for validation, and segments of same length obtained from the rest of the sequence will serve as training class. Feature distance between the validation sample and those of the training class is then calculated. This process is repeated for a number of times, and the value that exceeds 95% of the test samples is chosen as threshold.

Cross-validation technique is employed for threshold construction in both the AR spectrum distance plot and Mahalanobis distance plot presented herein.

5. Experimental validation of the statistical algorithms

For further verification of the statistical algorithms, they are also applied to acceleration data from two laboratory experiments. As in the numerical case, two acceleration datasets are obtained for either structural scenario.

5.1. Case study 1: truss model subjected to ambient vibrations.

Fig. 7 shows a picture of the specimen tested, with 14 wireless sensors mounted on the connection nodes. The truss is 1 m wide, 0.707 m tall, and has in the longitudinal direction four spans (lower cord), each 1.414 m long. For additional information on the truss, please see reference [34]. No additional excitation is applied except the ambient vibration, and two 20.4 kg disks are added to the mid-span of the truss to approximate a loss of stiffness in the system. For the undamaged case, the fundamental frequency estimate of the truss is 2.33 Hz. For the damaged case, the first frequency is 2.05 Hz.

The Ljung-Box test and statistical control charts have already been applied to free vibration data collected from the truss [34]. However, as the AR models were initially proposed as a tool to study stationary time series, it makes

Please cite this article as: R. Yao, S.N. Pakzad, Autoregressive statistical pattern recognition algorithms for damage detection in civil structures, Mech. Syst. Signal Process. (2012), doi:10.1016/j.ymssp.2012.02.014

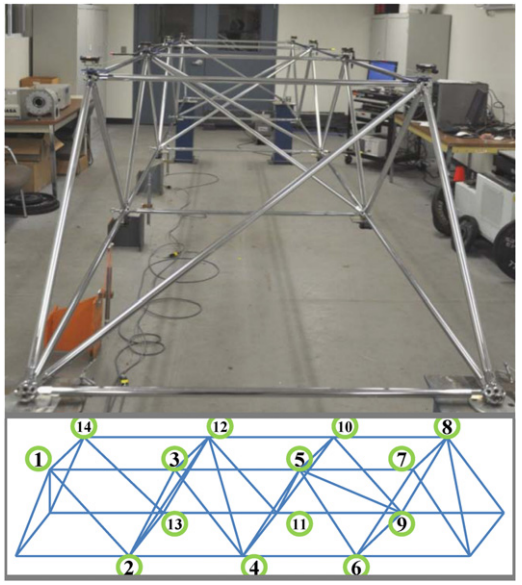

Fig. 7. The space truss model with its senor numbering scheme.

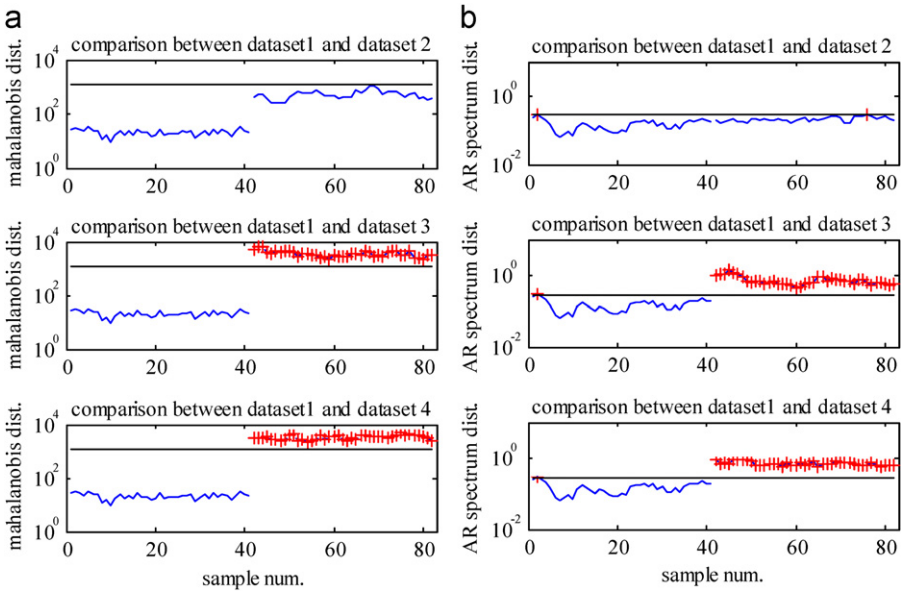

Fig. 8. Damage classification results for the space truss by (a) Mahalanabis distance and (b) Cosh spectral distance measure; all data are acquired from truss node 4.

more sense to apply them to ambient vibration responses. Due to the measurement noise disturbances in the high frequency content of the acceleration signals collected, the data is preprocessed using a low-pass filter before SPR evaluation. The results from Ljung-Box test, Mahalanobis distance and Cosh spectral distance evaluation are shown in Figs. 8 and 9. In all applications, the first two datasets are from healthy state, the rest from damaged state. The significance level of all thresholds is 5%. The maximum lag number for Q-statistic evaluation is 25. For evaluation of the Mahalanobis distance and Cosh spectral distance features, the AR model order selected to be 22, and each dataset is segmented into a group of 300-point long pieces with 250-point overlap between successive parts. The significance level of the threshold is 5%. The number of FFT (fast Fourier Transform) points is 256. Statistical control chart failed to yield a satisfactory classification result in this case. Again, the theoretical threshold of the Q-statistic generates false alarms.

Please cite this article as: R. Yao, S.N. Pakzad, Autoregressive statistical pattern recognition algorithms for damage detection in civil structures, Mech. Syst. Signal Process. (2012), doi:10.1016/j.ymssp.2012.02.014

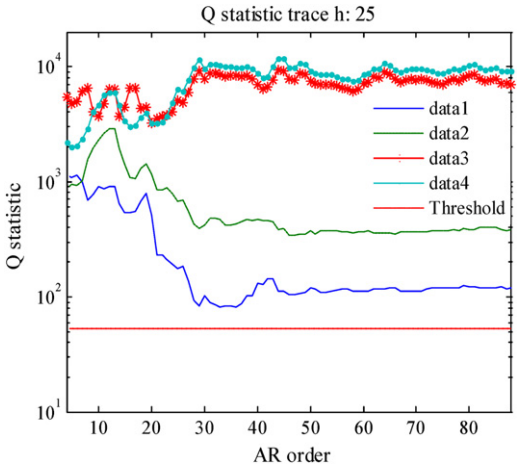

Fig. 9. Damage classification results for the space truss using Ljung-Box test statistic measure; All data are acquired from truss node 4.

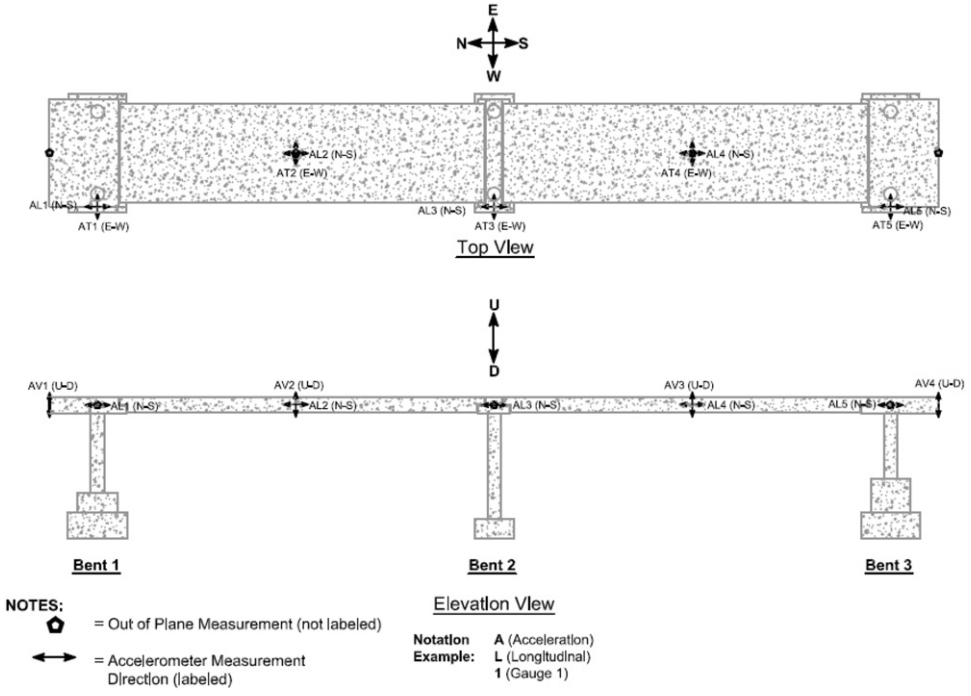

Fig. 10. Implementation of accelerometers on the bridge slab model [35].

5.2. *Case study 2: bridge slab model subjected to white-noise excitation*

The test specimen is a two-span reinforced concrete bridge model tested at the University of Nevada, Reno (Fig. 10). The three bents are each placed on separate shaking tables. Clear column heights of 1.83 m, 2.44 m, and 1.52 m were chosen for Bents 1, 2, and 3, and the diameter for each column is 0.31 m. The width and the total length of the slab were 2.5 m and 20.5 m. The design prototype was an idealized two-span frame of a cast-in-place, post-tensioned reinforced concrete box girder bridge. As part of a larger NEES (Network for Earthquake Engineering Simulation) project [35], the specimen was progressively damaged during various low-to-high amplitude level earthquake excitation tests, all of which were from the 90 degree and 180 degree components of the Century City Country Club North record from the 1994 Northridge, California earthquake. In the intervals between these tests, white noise excitation was applied to the structure. Minor cracks were first observed after the 13th earthquake test, and exposing of reinforcements

Please cite this article as: R. Yao, S.N. Pakzad, Autoregressive statistical pattern recognition algorithms for damage detection in civil structures, Mech. Syst. Signal Process. (2012), doi:10.1016/j.ymssp.2012.02.014

Table 2
Comparison of the performances of Mahalanobis distance and Cosh distance feature; misclassified cases are marked in bold.

		Outlier percentage			Inlier percentage			
		Dataset 1	Dataset 2		Dataset 3	Dataset 4		
Fig. 6	Mahalanobis	0.00%	**9.26%**		27.78%	29.63%		
	Cosh	3.70%	**7.41%**		27.78%	46.30%		
		Dataset 1	Dataset 2		Dataset 3	Dataset 4		
Fig. 8	Mahalanobis	0.00%	0.00%		0.00%	0.00%		
	Cosh	0.00%	2.44%		0.00%	0.00%		
		WN0709B	WN0709A	WN1112A	WN1415	WN1718	WN1819	WN1920
Fig. 11	Mahalanobis	0.00%	**38.71%**	**37.63%**	0.00%	0.00%	0.00%	0.00%
	Cosh	2.15%	**12.90%**	3.23%	22.58%	0.00%	0.00%	0.00%

Table 3
Damage progression summary for each bent [35].

Test	Observed damage		
	Bent 1	Bent 2	Bent 3
12	–	–	–
13	CRACK (0.08)	–	–
14	CRACK (0.08)	CRACK (0.08)	CRACK (0.08)
15	CRACK (0.25), FL	CRACK (0.08)	CRACK (0.25),SPAL (100)
16	CRACK (0.50),SPAL (125)	CRACK (0.17), FL	CRACK (0.33),SPAL (100), TranEXP
17	CRACK (0.50),SPAL (150), TranEXP	CRACK (0.25), FL	CRACK (0.50),SPAL (100), TranEXP
18	CRACK (0.50),SPAL (150), TranEXP	CRACK (0.50),SPAL (100)	CRACK (2.00),SPAL (140), TranEXP, LongEXP, InBUCK
19	CRACK (0.75),SPAL (150), TranEXP	CRACK (2.00),SPAL (115)	CRACK (2.00),SPAL (150), TranEXP, LongEXP, BUCK, TranFRAC
20	CRACK (0.75),SPAL (150), TranEXP, LongEXP	CRACK (2.00),SPAL (125)	CRACK (2.00),SPAL (150), TranEXP, LongEXP, BUCK, TranFRAC, LongFRAC
21	CRACK (0.75),SPAL (150), TranEXP, LongEXP	CRACK (2.00),SPAL (125)	CRACK (2.00),SPAL (150), TranEXP, LongEXP, BUCK, TranFRAC, LongFRAC, CORE
22	CRACK (0.75),SPAL (150), TranEXP, LongEXP, InBUCK	CRACK (2.00),SPAL (200), TranEXP, BUCK	CRACK (2.00),SPAL (150), TranEXP, LongEXP, BUCK, TranFRAC, LongFRAC, CORE

Notes: BUCK—buckling of longitudinal reinforcement, CORE—complete core degradation, CRACK—crack width in mm, InBUCK—incipient buckling, LongEXP—the exposing of longitudinal reinforcement, LongFRAC—fracture of the longitudinal reinforcement, SPAL—spall height in mm, TranEXP—the exposing of transverse reinforcement, TranFRAC—fracture of the transverse reinforcement.

occurred after 15th test, other details on the damage accumulation in bridge bents can be found in Table 3. The data used here is the transverse acceleration measurements of the slab from white-noise tests collected from sensor AT3 (Fig. 10). The names of the data files, as shown in Figs. 11 to 13, is a combination of the number of the earthquake tests before and after the white noise test, with common prefix 'WN'. Postfixes are employed to distinguish data from different tests under same structural condition.

For all the results presented for this case study, the first three datasets are from the healthy state, the rest from the damaged state. Again, thresholds with a 5% significance level are used for all features. When evaluating the Mahalanobis distance and Cosh spectral distance, the AR model order used is 20, and each dataset is segmented into a group of 350-point long pieces with 300-point overlap between successive parts. The number of FFT (Fast Fourier Transform) points is 256. The AR model order used in control chart construction is 15, and the subgroup size is 10. It is observed that when the damage is small, features calculated from model coefficients are no less sensitive than those from residuals. But when the damage becomes severer, the value of latter increases much more rapidly than the former. This can be explained by the results presented in Section 3: the change in autocorrelation/variance is the sum of pole shifts and a number of second order terms with possibly small denominator values. The 'second order effect' will grow prominent when the damage becomes more substantial. The statistical control method performs quite well in this case, possibly because the excitation is a controlled white noise input.

Also, it can be observed in all of the numerical and experimental applications the Cosh distance outperforms the Mahalanobis distance in that the former is relatively more robust to excitation condition variations. The percentages of outliers/inliers of the application examples are provided in Table 2. Note that for all the figures the threshold is set at a 5% statistical significance level, which means damage is recognized when the outlier portion exceeds 5% of the total observations (or equivalently, when the inlier portion falls below 95% of the total observations). It is clear that the Cosh spectral distance yields a more consistent performance for the baseline and false-positive testing datasets, while remains overall sensitive to structural damage.

It is worth noting that as the system becomes non-linear, many feature values stop reflecting the damage extent, due to the invalidity of LTI (linear time invariant) assumption for the system.

Please cite this article as: R. Yao, S.N. Pakzad, Autoregressive statistical pattern recognition algorithms for damage detection in civil structures, Mech. Syst. Signal Process. (2012), doi:10.1016/j.ymssp.2012.02.014

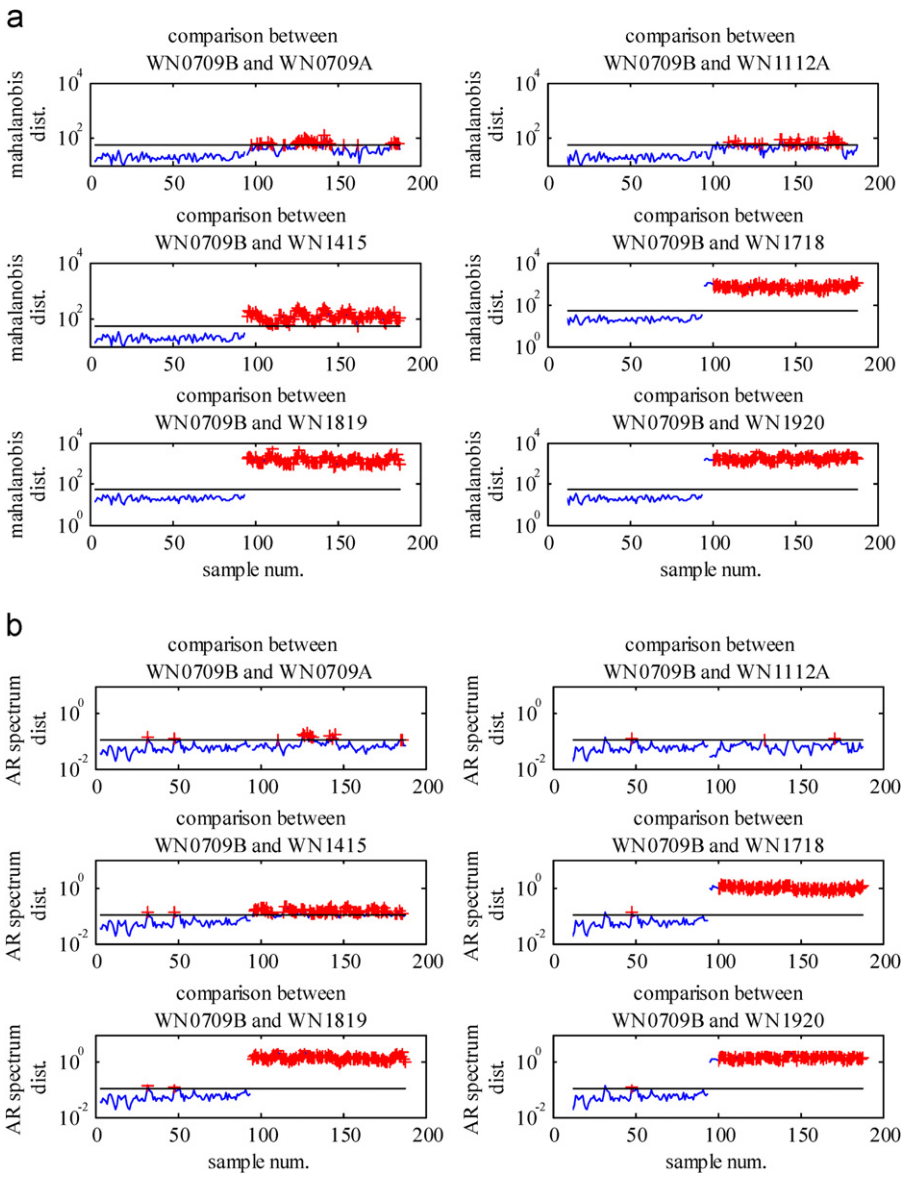

Fig. 11. Damage classification results for the bridge slab model by (a) Mahalanobis distance and (b) Cosh spectral distance measure; all data are acquired from node 3.

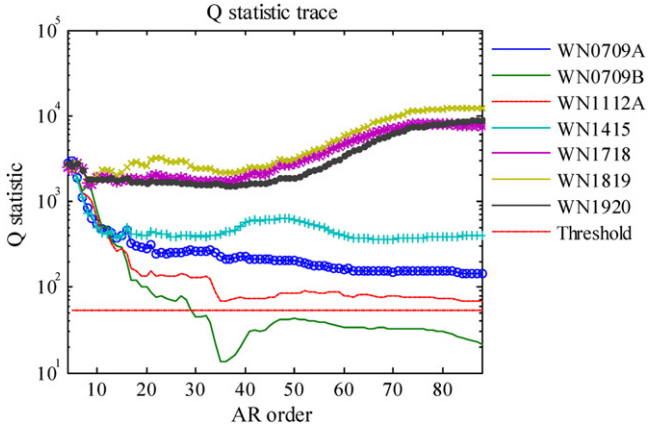

Fig. 12. Damage classification results for the bridge slab model using Ljung-Box test statistic measure; the maximum lag number for *Q*-statistic evaluation is 25.

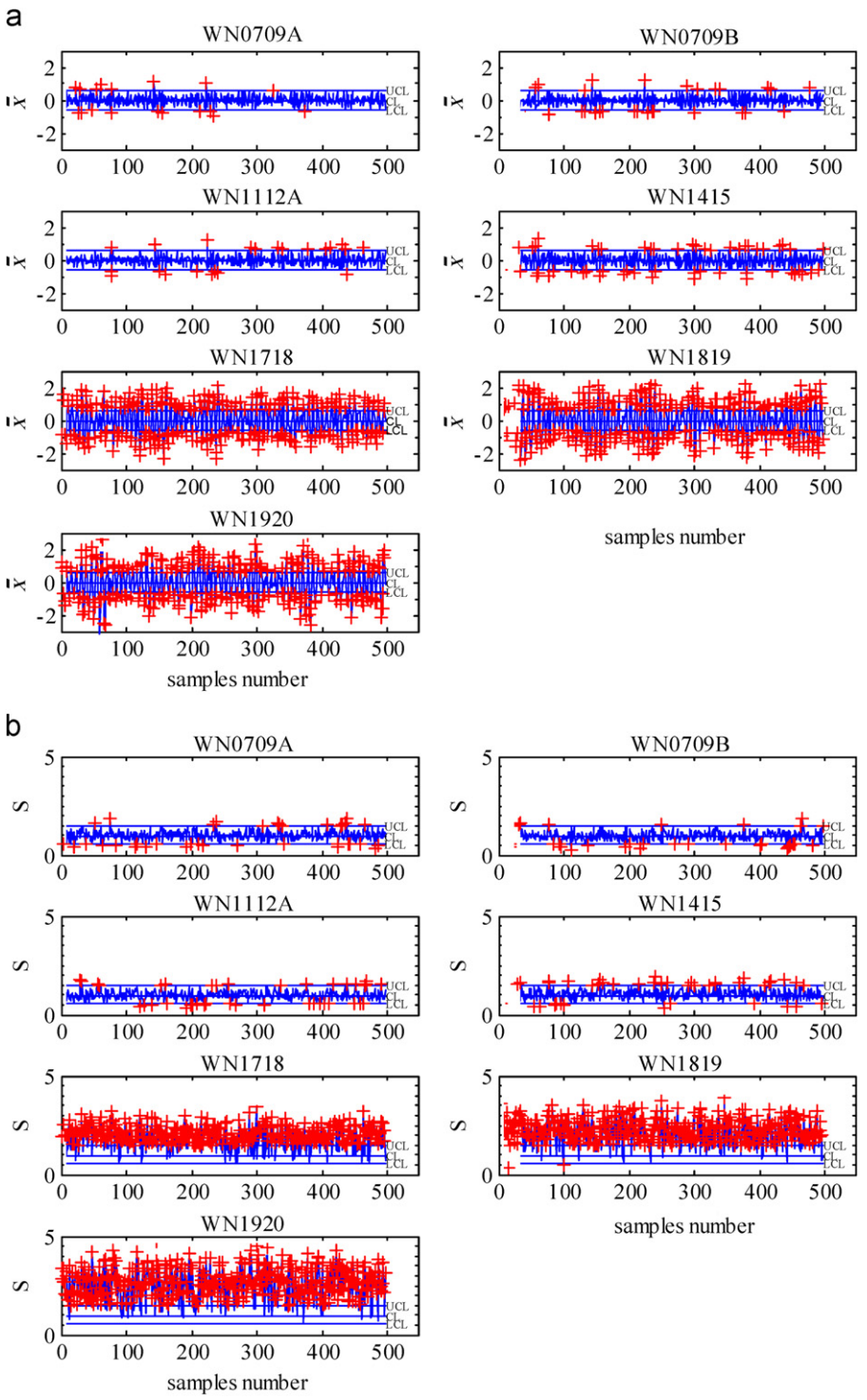

Fig. 13. Damage classification results for the bridge slab model, by (a) $\bar{x}$ control chart and (b) S-control chart measure; data set WN0709B is employed as baseline here. all data are acquired from node 3.

6. Conclusion

In this paper, two time series-based structural damage detection algorithms using statistical pattern recognition are proposed and investigated. One of them uses the Ljung-Box statistic of AR model residual sequence as damage index; the

Please cite this article as: R. Yao, S.N. Pakzad, Autoregressive statistical pattern recognition algorithms for damage detection in civil structures, Mech. Syst. Signal Process. (2012), doi:10.1016/j.ymssp.2012.02.014

other uses the Cosh spectral distance of the estimated AR model spectrum. Compared with existing algorithms based on AR model residual variance and coefficients distance, the Ljung-Box statistic provides a more accurate account of the structural damage by evaluating possible change in the entire ACF of residuals and Cosh spectral distance is less sensitive to changes in excitation sources as its value is largely determined by system poles, a property shared by most spectrum-based features. Subsequent applications to vibration data from simulation and lab experiments shows that the Ljung-Box statistic is indeed a more sensitive feature than residual variance in most cases, while Cosh spectral distance tends to be more stable than Mahalanobis distance of coefficients.

In all the applications presented, the theoretical threshold of Ljung-Box test is conservative (i.e., generates a large number of false positives). The available control chart method also suffers from similar threshold construction inaccuracies. This problem arises from the fact that the structural response is not precisely an AR process, and the residuals obtained from the estimated model are not exactly white noise as assumed in the formulation of the Ljung-Box test. This discrepancy between the theoretical results and those from real data is inevitable because of statistical modeling errors. The data- driven resampling method proposed for threshold construction for Mahalanobis distance and Cosh spectral distance measure yields a better performance. Here the cross-validation technique is selected for threshold determination over Monte Carlo method because the latter's assumption that the AR model coefficients are Gaussian random vectors with statistically independent components is not theoretically sound. Similar procedures may also be attempted for the residual based features in future research.

References

[1] C.F. Farrar, K. Worden, An introduction to structural health monitoring, Philos. Trans. R. Soc. A 365 (1851) (2007) 303–315.
[2] D. Bernal, Load vectors for damage localization, J. Eng. Mech. 128 (1) (2002) 7–14.
[3] S.W. Doebling, C.R. Farrar, M. Prime, A summary review of vibration-based damage identification methods, Shock and Vibration Digest 30 (2) (1998) 91–105.
[4] N. Haritos, J.S. Owen, The use of vibration data for damage detection in bridges: a comparison of system identification and pattern recognition approaches, Struct. Health Monit. 3 (2) (2004) 141–163.
[5] M.M.A. Wahab, Parameterization of damage in reinforced concrete structures using model updating, J. Sound Vib. 228 (4) (1999) 717–730.
[6] A.K. Jain, R.P.W. Duin, J. Mao, Statistical pattern recognition: a review, IEEE Trans. Pattern Anal. Mach. Intell. 22 (1) (2000) 4–37.
[7] T.K. Ho, H.S. Baird, Large-scale simulation studies in image pattern recognition, IEEE Trans. Pattern Anal. Mach. Intell. 19 (10) (1997) 1067–1079.
[8] F. Jelinek, Continuous speech recognition by statistical methods, Proc. IEEE 64 (4) (1976) 532–556.
[9] J. Schurmann, N. Bartneck, T. Bayer, J. Franke, E. Mandler, M. Oberlander, Document analysis-from pixels to contents, Proc. IEEE 80 (7) (1992) 1101–1119.
[10] A.W. Liew, H. Yan, M. Yang, Pattern recognition techniques for the emerging field of bioinformatics: a review, Pattern Recognit. 38 (11) (2005) 2055–2073.
[11] Farrar, C.R., Duffey, T.A., Doebling, S.W., Nix, D.A. 1999. A statistical pattern recognition paradigm for vibration-based structural health monitoring, 2nd International Workshop on Structural Health Monitoring, Stanford, CA.
[12] M.L. Fugate, H. Sohn, C.R. Farrar, Vibration-based damage detection using statistical process control, Mech. Syst. Sig. Process. 15 (4) (2001) 707–721.
[13] H. Sohn, C.R. Farrar, Damage diagnosis using time series analysis of vibration signals, Smart Mater. Struct. Vol.10 (No 3) (2001) 446–452.
[14] H. Sohn, C.R. Farrar, N.F. Hunter, K. Worden, Structural health monitoring using statistical pattern recognition techniques, J. Dyn. Syst. Meas. Contr. 123 (4) (2001) 706–711.
[15] H. Sohn, K. Worden, C.R. Farrar, Statistical damage classification under changing environmental and operational conditions, J. Intell. Mater. Syst. Struct. 13 (9) (2002) 561–574.
[16] O.R. De Lautour, P. Omenzetter, Nearest neighbor and learning vector quantization classification for damage detection using time series analysis, Struct. Control Health Monit. 17 (6) (2010) 614–631.
[17] J.S. Sakellariou, S.D. Fassois, Stochastic output error vibration-based damage detection and assessment in structures under earthquake excitation, J. Sound Vib. 297 (3–5) (2006) 1048–1067.
[18] P.J. Brockwell, R.A. Davis, Time Series: Theory and Methods, 2nd edn., Springer, NY, 2009.
[19] P.J. Brockwell, R.A. Davis, Introduction to Time Series and Forcasting, 2nd edn., Springer, NY, 2002.
[20] J.B. Bodeux, J.C. Golinval, Application of ARMAV models to the identification and damage detection of mechanical and civil engineering structures, Smart Mater. Struct. 10 (3) (2001) 479–489.
[21] Y. Lu, F. Gao, A novel time-domain auto-regressive model for structural damage diagnosis, J. Sound Vib. 283 (3–5) (2005) 1031–1049.
[22] H.Y. Noh, K.K. Nair, A.S. Kiremidjian, C.H. Loh, Application of time series based damage detection algorithms to the Benchmark experiment at the National Center for Research on Earthquake Engineering (NCREE) in Taipei, Taiwan, Smart Struct. Syst. 5 (1) (2009) 95–117.
[23] P. Omenzetter, J.M.W. Brownjohn, Application of time series analysis for bridge monitoring, Smart Mater. Struct. 15 (1) (2006) 129–138.
[24] H. Zheng, A. Mita, Localized damage detection of structures subject to multiple ambient excitations using two distance measures for autoregressive models, Struct. Health Monit. 8 (3) (2009) 207–222.
[25] M. Gul, F.N. Catbas, Statistical pattern recognition for structural health monitoring using time series modeling: theory and experimental verifications, Mech. Syst. Sig. Process. 23 (Issue 7) (2009) 2192–2204.
[26] S.D. Fassois, J.S. Sakellariou, Time series methods for fault detection and identification in vibrating structures, Philos. Trans. R. Soc. A 365 (1851) (2007) 411–448.
[27] K.K. Nair, S.K. Anne, K.H. Law, Time series-based damage detection and localization algorithm with application to the ASCE Benchmark structure, J. Sound Vib. 291 (Issues 1–2) (2006) 349–368.
[28] H. Zheng, A. Mita, Two-stage damage diagnosis based on the distance between ARMA models and pre-whitening filters, Smart Mater. Struct. 16 (5) (2007) 1829–1836.
[29] K. Worden, G. Manson, The application of machine learning to structural health monitoring, Philos. Trans. R. Soc. A 365 (1851) (2007) 515–537.
[30] P.C. Mahalanobis, On the generalized distance in statistics, Proc. Nat. Inst. Sci. India 2 (1) (1936) 49–55.
[31] A.V. Oppenheim, R.W. Schafer, Discrete-Time Signal Processing, 3rd edn., Prentice Hall, NJ, 2009.
[32] G.M. Ljung, G.E.P. Box, On a measure of lack of fit in time series models, Biometrika 65 (2) (1978) 297–303.
[33] B. Wei, J.D. Gibson, Comparison on distance measures in discrete spectral modeling, Proc. IEEE Digital Signal Process. Workshop (2000) 1–4.
[34] Dorvash, S., Yao, R., Pakzad, S.N. and Okaly, K., 2010, Static and dynamic model validation and damage detection using wireless sensor network, The 5th International Conference on Bridge Maintenance, Safety & Management, Philadelphia, PA.
[35] N. Johnson, R.T. Ranf, M.S. Saiidi, D. Sanders, M. Eberhard, Seismic testing of a two-span reinforced concrete bridge, J. Bridge Eng. 13 (2) (2008) 173–182.

Please cite this article as: R. Yao, S.N. Pakzad, Autoregressive statistical pattern recognition algorithms for damage detection in civil structures, Mech. Syst. Signal Process. (2012), doi:10.1016/j.ymssp.2012.02.014